Microbial decomposition of marine dissolved organic matter in cool oceanic crust

Sunita R. Shah Walter[1,2,6]*, Ulrike Jaekel[1,7], Helena Osterholz[3], Andrew T. Fisher[4], Julie A. Huber [5], Ann Pearson[2], Thorsten Dittmar[3]* and Peter R. Girguis[1]*

Marine dissolved organic carbon (DOC) is one of the largest active reservoirs of reduced carbon on Earth. In the deep ocean, DOC has been described as biologically recalcitrant and has a radiocarbon age of 4,000 to 6,000 years, which far exceeds the timescale of ocean overturning. However, abiotic removal mechanisms cannot account for the full magnitude of deep-ocean DOC loss. Deep-ocean water circulates at low temperatures through volcanic crust on ridge flanks, but little is known about the associated biogeochemical processes and carbon cycling. Here we present analyses of DOC in fluids from two borehole observatories installed in crustal rocks west of the Mid-Atlantic Ridge, and show that deep-ocean DOC is removed from these cool circulating fluids. The removal mechanism is isotopically selective and causes a shift in specific features of molecular composition, consistent with microbe-mediated oxidation. We suggest organic molecules with an average radiocarbon age of 3,200 years are bioavailable to crustal microbes, and that this removal mechanism may account for at least 5% of the global loss of DOC in the deep ocean. Cool crustal circulation probably contributes to maintaining the deep ocean as a reservoir of 'aged' and refractory DOC by discharging the surviving organic carbon constituents that are molecularly degraded and depleted in ^{14}C and ^{13}C into the deep ocean.

N orth Pond is a sediment-covered bathymetric depression located below the oligotrophic Sargasso Sea at ~4,450 m water depth. It sits on 8-Myr-old volcanic crust, along the western flank of the Mid-Atlantic Ridge[1,2] (Fig. 1a,b). North Pond has a long history of oceanographic surveys and drilling studies, and is instrumented with several sealed borehole observatories (CORKs (Circulation Obviation Retrofit Kits))[3]. Heat-flow studies, CORK data and sediment core data suggest that large volumes of seawater are drawn down into the porous and permeable upper basaltic crust through unsedimented outcrops, and flow laterally through the crust beneath low-permeability sediments. This vigorous flow removes 70–90% of the heat flux predicted by lithospheric models[4–6]. Fluids recovered from the upper 300 m of the crustal 'aquifer' are oxygenated, cooler than 20 °C and have an inorganic chemical composition that strongly resembles bottom seawater[7,8]. Active microbial communities were also found in recovered borehole fluids[7]. The crustal aquifer below North Pond can be thought of as a continuous-flow bioreactor provisioned with organic carbon and inoculated with microbial populations from oceanic bottom water. Accordingly, the North Pond CORKs offer unique windows into a natural experiment in which the fate of marine dissolved organic carbon (DOC) can be examined in the expansive, cool crustal hydrothermal system.

Fluids were sampled in 2012 and 2014 from one depth in the shallow crust at IODP (Integrated Ocean Drilling Program) Hole U1382A, and from three crustal depths in Hole U1383C (Fig. 1b,c). Geochemical, microbiological and heat-flow data all indicate a greater connectivity between the open ocean and Hole U1382A compared to U1383C (refs [4,7]). The gradient from the open ocean to increasing isolation within the basalt-hosted subsurface is evident in dissolved oxygen, which is highest in the bottom water[8], has intermediate values at Hole U1382A and is lowest at the three depths of U1383C (Fig. 2a)[7,8]. Although some loss of dissolved oxygen can be attributed to upward diffusion into the overlying sediments, modelling shows that reactive losses are also required[9], which implies the oxidation of organic carbon or reduced minerals within the crust.

Radiocarbon-based estimates of fluid residence time

Dissolved inorganic carbon (DIC) in crustal fluid samples is depleted in ^{14}C relative to the bottom seawater (Fig. 3a, squares). In this aquifer, contact with the basaltic crust seems to have caused minimal to no alteration to the DIC reservoir [7]. As such, we can use its radiocarbon content as a proxy for incubation time within the subsurface. Recognizing that these estimates are influenced by the combined effects of radiocarbon decay and loss of ^{14}C-enriched DIC through diffusion and mixing with more stagnant fluids, we estimate an average apparent incubation time of 350 ± 100 radiocarbon years at Hole U1382A, and a time- and depth-averaged incubation time of $2,400 \pm 300$ years at Hole U1383C (where reported uncertainties account for the potential influence of oxidized organic carbon on the crustal DIC reservoir (Table 1 and Supplementary Sections 1.1 and 1.2)). Although heat-flow measurements indicate a rapid lateral flow of cool fluids through well-connected subsurface channels beneath North Pond[5,6], consistent with the 1–10 year residence time estimate for global hydrothermal fluids[10], such measurements are biased towards fluids that flow efficiently through subsurface channels[11]. With incubation times 10–100-fold longer, our samples may, instead, represent the heterogeneity of the crustal environment,

[1]Department of Organismic and Evolutionary Biology, Harvard University, Cambridge, MA, USA. [2]Department of Earth and Planetary Sciences, Harvard University, Cambridge, MA, USA. [3]Institute for Chemistry and Biology of the Marine Environment (ICBM), University of Oldenburg, Oldenburg, Germany. [4]Earth and Planetary Sciences Department, University of California, Santa Cruz, Santa Cruz, CA, USA. [5]Marine Chemistry and Geochemistry, Woods Hole Oceanographic Institution, Woods Hole, MA, USA. [6]Present address: School of Marine Science and Policy, College of Earth, Ocean, and Environment, University of Delaware, Lewes, MA, USA. [7]Present address: The Research Council of Norway, Oslo, Norway. *e-mail: suni@udel.edu; thorsten.dittmar@uni-oldenburg.de; pgirguis@oeb.harvard.edu
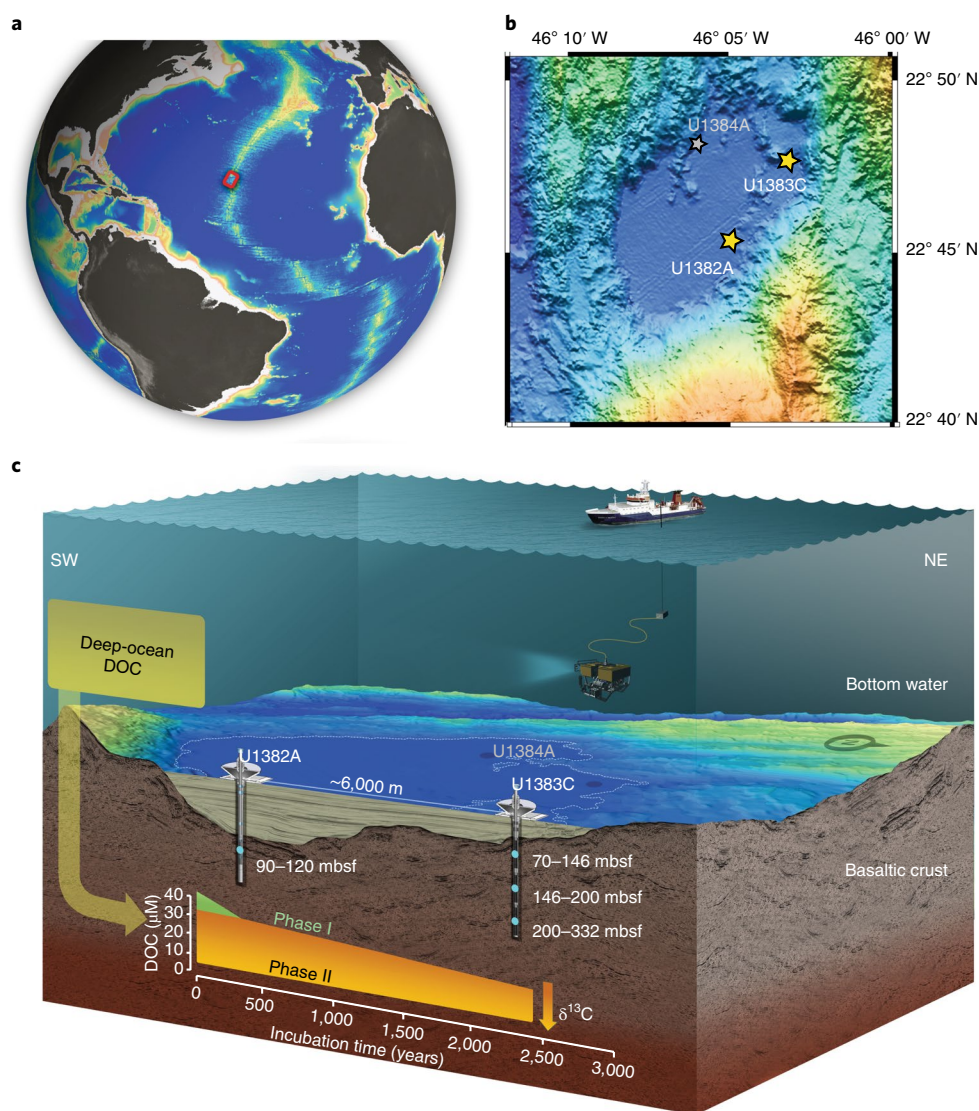
Fig. 1 | Sampling locations and schematic representation of the DOC transformation within the crust at the North Pond IODP study site. a, Locations of CORK installations on the western flank of the Mid-Atlantic Ridge. **b**, Bathymetry of North Pond and the surrounding outcrops[2]. **c**, Model of how bottom seawater migrates into the crust from bare outcrops and flows laterally through the relatively porous crust. Entrained DOC is removed in two phases: phase I, during which 7–10 μM DOC of approximately modern age is removed at 0.02 μM yr⁻¹, and phase II, during which approximately 10 μM DOC with average radiocarbon age of 3,200 years is removed at 0.008 μM yr⁻¹.

which includes the diffusion and mixing of ^{14}C-depleted DIC from slower, more convoluted flow paths and stagnant zones.

Seawater origin of SPE-DOM in subsurface fluids

The molecular composition of dissolved organic matter (DOM) solid-phase extracted (SPE) on styrene-divinyl benzene resin[12] (SPE-DOM) from crustal fluids, bottom water and pore water from overlying sediments was assessed via Fourier-transform ion cyclotron resonance mass spectrometry (FT-ICR-MS), an ultrahigh-resolution mass spectrometry technique[13,14,15]. Qualitatively, the spectra of the detected molecular masses from crustal fluid SPE-DOM bear a striking resemblance to the bottom water SPE-DOM (Supplementary Fig. 1). Cluster analysis of the relative FT-ICR-MS signal intensities based on Bray–Curtis dissimilarities shows that the crustal aquifer fluids cluster with bottom water, distinct from a separate group that represent pore-water samples from nearby sediments (Supplementary Fig. 2). Molecular composition (Supplementary Figs. 1–3), therefore, supports a seawater origin for the standing stock of crustal SPE-DOM with a minimal influence from sedimentary pore water.

Selective microbial removal of DOC and SPE-DOM

DOC and dissolved oxygen concentrations from bottom seawater, Hole U1382A and all three depths at Hole U1383C are strongly correlated for the fluids collected in both 2012 and 2014 (Supplementary Fig. 4), which suggests that oxidation of DOC may be an important sink for oxygen in the oxygenated subsurface. The ratio between DOC and oxygen consumption, however, is 0.34, much lower than the Redfield Ratio predicts (0.69) (ref. [16]). Although some of this difference can be attributed to oxygen loss via upward diffusion into sediments[9], an additional reactive sink for dissolved oxygen is also possible. DIC in crustal fluids has δ^{13}C values (average of $+0.35 \pm 0.3$‰) that are slightly negative relative to that of bottom seawater ($+1.0$‰) and therefore also appear to be influenced by organic carbon oxidation (Fig. 3b). Isotopic mass balance indicates that these relatively negative δ^{13}C values require 30–120 ($\pm$50) μM of DIC from oxidized organic carbon, more than can be accounted for by DOC oxidation alone (Supplementary Section 1.2). The decrease in DOC concentrations within the crust is, at most, 23 ± 2 μM. Particulate organic carbon from the deep-ocean bottom water,
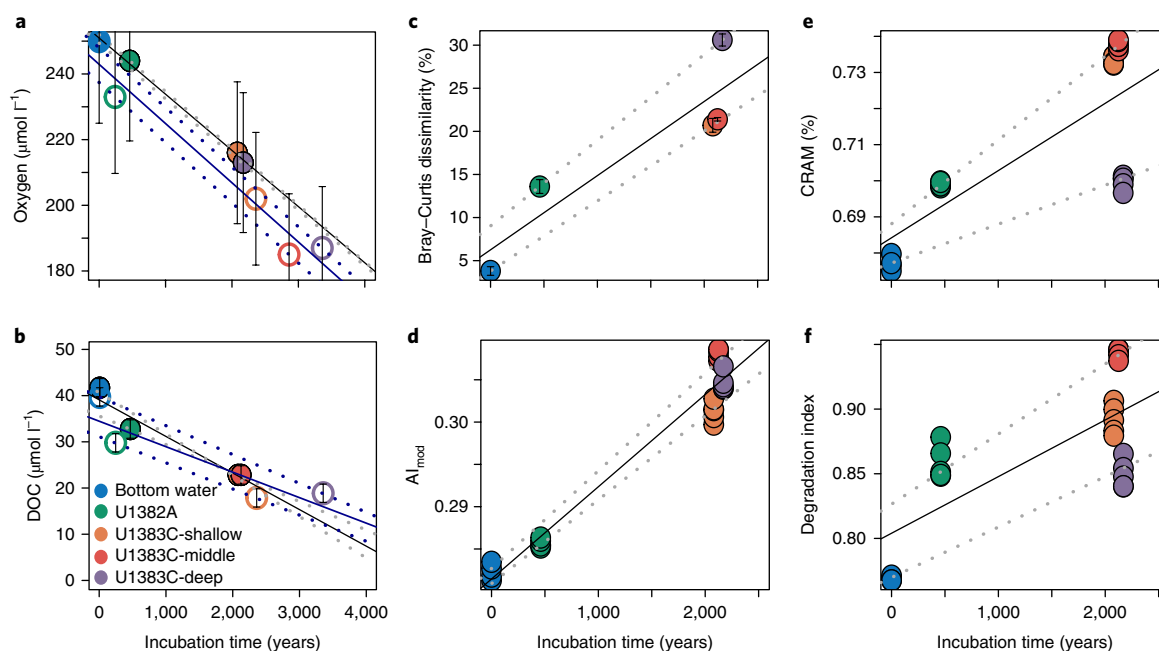
Fig. 2 | Concentrations of dissolved oxygen and DOC with SPE-DOM molecular composition indices versus incubation time in the North Pond crustal aquifer. a, Bottom water[8] and crustal oxygen concentrations of dissolved oxygen[7] from samples collected in 2012 (filled) and 2014 (open). **b**, DOC concentrations from 2012 (filled) and 2014 (open). Error bars in **a** and **b** denote the measurement uncertainty. **c–f**, Molecular composition indices: Bray–Curtis dissimilarities calculated against the bottom water (circles, average dissimilarity; error bars, s.d. of replicate analyses) (**c**), AI$_{mod}$ (refs [13,19]) (**d**), proportion of CRAM[23] (**e**) and degradation index[14] (**f**). Same-coloured symbols denote replicate analyses in **d–f**. Black lines, least squares estimate; dotted grey lines, 25% and 75% quantile regressions. The incubation time for U1383C middle is the average of the shallow and deep incubation times from 2012.

augmented with particles entrained at the seafloor during recharge, could be an important, although unconstrained, source of reduced carbon to the crustal aquifer. Regardless, both scenarios indicate that DOC is removed within the crust by oxidation rather than by other processes, such as adsorption to mineral surfaces[17,18].

Δ^{14}C values of DOC in crustal fluids reflect the combined effects of radiocarbon decay, diffusion and mixing with ^{14}C-depleted DOC from stagnant zones, isotopically selective DOC oxidation and contributions from in situ sources. The importance of processes other than decay and mixing with aged stagnant fluids is attested by molecular-level changes observed within SPE-DOM[15]. Despite the overall similarity maintained between seawater and crustal

fluid SPE-DOM (Supplementary Figs. 1–3), as DOC concentration decreases (Fig. 2b), the increases in Bray–Curtis dissimilarity (Fig. 2c), modified aromaticity index (AI$_{mod}$) (Fig. 2d)[13,19] and degradation index (Fig. 2f)[14] document a progressive alteration of subsurface SPE-DOM (Supplementary Fig. 5).

To isolate the isotopic signature of DOC transformations separately from the effects of radiocarbon decay, we subtracted DIC-based incubation times (Table 1) from the measured radiocarbon ages of each DOC sample and converted the resulting corrected ages to Δ^{14}C values (Table 1 and Supplementary Section 2.4). Except for the deepest horizon at Hole U1383C, all the age-corrected Δ^{14}C values are more negative than DOC in the Sargasso Sea bottom

Table 1 | Carbon isotopic composition of DIC and DOC in the North Pond aquifer

Sample description	Year sampled	DIC								DOC									
		δ¹³C (‰)	±	Δ¹⁴C (‰)	±	Age (yr)	±	Incubation time (yr)	±	Concentration (μM) ±2	δ¹³C (‰)	±	Δ¹⁴C (‰)	±	Age (yr)	±	Age-corrected Δ¹⁴C (‰)	±
Bottom water	2014	1.0	0.1	−110	2	870	20	0		41	−23.3	0.5	−447	2	4,690	20		
U1382A 90–120 mbsf	2012	0.67	0.1	−158	2	1,330	20	460	60	33	−24.7	0.5	−607	2	7,440	30	−581	4
	2014	0.43	0.1	−135	2	1,100	20	240	100	30	−23.9	0.5	−528	2	5,970	30	−511	7
U1383C 70–146 mbsf	2012	−0.16	0.1	−308	2	2,900	30	2100	300	23	−25.2	0.5	−684	2	9,200	50	−590	10
	2014	0.53	0.1	−331	2	3,170	30	2400	100	18	−24.1	0.5	−622	2	7,760	40	−493	7
U1383C 146–200 mbsf	2012	n.d.		n.d.		n.d.		n.d.		23	−26.6	0.5	−678	2	9,040	50	−578	6
	2014	n.d.		n.d.		n.d.		n.d.		n.d.	n.d.		n.d.		n.d.		n.d.	
U1383C 200–332 mbsf	2012	0.53	0.1	−315	2	2,980	30	2200	100	n.d.	n.d.		n.d		n.d		n.d.	
	2014	0.1	0.1	−407	1	4,130	20	3400	300	19	−24.7	0.5	−602	2	7,340	30	−400	20

δ¹³C Vienna PeeDee Belemnite. Δ¹⁴C calculated according to a published method[32]. n.d., not determined.
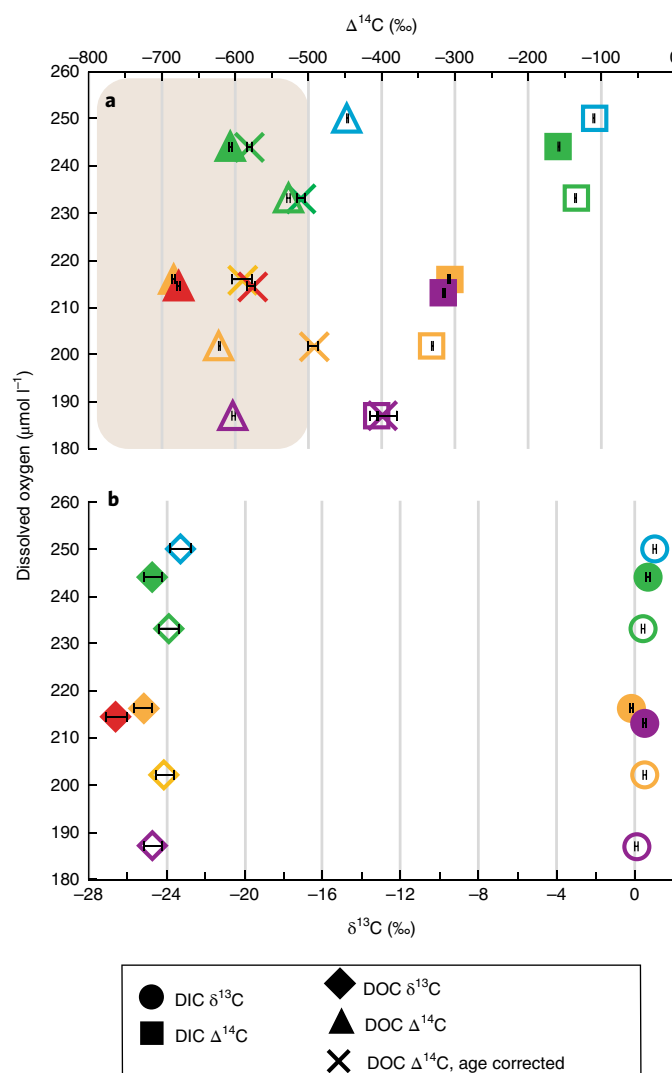
Fig. 3 | Isotopic composition of bottom water and crustal DIC and DOC at North Pond. a,b, Measured $\Delta^{14}C$ (**a**) and $\delta^{13}C$ (**b**) values of DIC and DOC from bottom water (blue) and crustal fluids U1382A (green), U1383C shallow (orange), middle (red) and deep (purple) for samples collected in 2012 (filled) and 2014 (open) plotted against dissolved oxygen concentrations[78] as a proxy for increasing isolation within the crustal aquifer. Error bars denote the measurement uncertainty. The range of reported $\Delta^{14}C$ values for methane-hydrate-associated DOC[33] and Juan de Fuca Ridge Flank DOC[34] are shaded in brown. Our DOC $\Delta^{14}C$ values resemble hydrothermal fluids and methane-hydrate fluids[33], but neither is a suitable model for North Pond.

water, that is, they show excess ^{14}C depletion. However, no trend is apparent with increasing time within the crust (Fig. 3a, crosses), arguing against the accumulation of isotopically distinct chemosynthetic or sedimentary DOC. DOC loss after ~350 years also does not appear to be ^{14}C selective. The initial rate of DOC loss is faster (0.02 μM yr^{-1}) in the first ~350 years compared to the cumulative rate of loss over ~2,400 years (average 0.008 μM yr^{-1}). The fraction of DOC removed first also has a greater median radiocarbon age (2,500–4,300 (±1,000) years) than the fraction removed over ~2,400 years (modern to 2,500 (±2,000) years (Supplementary Section 2.5). Together, these results are consistent with the earlier removal of semilabile DOC sourced from a deep-ocean subreservoir described as ^{14}C enriched and turning over quickly relative to bulk DOC[20], followed by a slower removal of more aged refractory components. The coarse temporal resolution of our samples also allows that the removal of the more labile fraction of DOC in the crust could occur on a timescale shorter than ~350 years, possibly similar to the decadal timescale estimated for deep-ocean semilabile DOC[20].

Crustal DOC has $\delta^{13}C$ values that are more negative than seawater DOC (Fig. 3b). With increasing measured DOC radiocarbon

age, we observe a shift towards increasingly negative DOC $\delta^{13}C$ values (Supplementary Fig. 6). This trend indicates that the subsurface DOC removal processes prefer components that are more ^{13}C enriched. Kinetic isotope fractionation during biosynthesis results in lipids being ^{13}C depleted compared to proteins and carbohydrates[21,22]. Although proteins, carbohydrates and lipids themselves are not detected in crustal SPE-DOM, molecules that contain these moieties could retain the isotopic imprint of their respective biosynthetic pathways. The preferential preservation of DOC components derived from lipid synthesis pathways provides a plausible mechanism to explain these isotopic and molecular results. For example, carboxyl-rich alicyclic molecules (CRAMs) have been identified as a class of molecules within deep-sea DOC that is particularly resistant to degradation, and share structural characteristics with polycyclic isoprenoid lipids[23]. Isoprenoid lipids are depleted in ^{13}C relative to biomass[21], which suggests that CRAM molecules should also be relatively ^{13}C depleted. The selective preservation of CRAM in the crustal aquifer is indicated by SPE-DOM molecular composition (Fig. 2e) and could contribute to the observed pattern in $\delta^{13}C$ values.

Our evidence points towards microbe-mediated oxidation as the dominant process responsible for DOC transformation and the selective removal of specific DOC fractions in the cool crustal subsurface. Heterotrophic discrimination between isotopically dissimilar sources of DOC has been observed in other marine and aquatic environments[24,25], which is consistent with our observations. Metabolic selectivity of heterotrophic microbes is probably important in determining the overall fate of marine DOC, and these data suggest that the microbial communities in low-temperature crustal aquifers are of global geochemical importance.

Chemoautotrophic production of DOC within the crust

Microbial assemblages recovered from North Pond samples show both heterotrophic and chemoautotrophic potential[7,8]. The production of chemosynthetic DOC in crustal fluids below North Pond would incorporate relatively ^{14}C-enriched DIC and lead to more-positive DOC $\Delta^{14}C$ values, which is contrary to our observations for U1382A and the shallower horizons at U1383C (Fig. 3a). In the shallow crustal fluids, isotopic evidence suggests that, if substantial chemosynthetic DOC is produced in situ, it must be quickly recycled so as not to influence the standing inventory of subsurface DOC. At the deepest horizon at U1383C, however, the age-corrected DOC $\Delta^{14}C$ value is significantly 'younger' than all other age-corrected values, and more positive than bottom-water DOC, which suggests a net contribution of ^{14}C-enriched DOC potentially from chemoautotrophy. Deep SPE-DOM also shows the greatest Bray–Curtis dissimilarity from other crustal fluids and bottom water (Fig. 2c and Supplementary Figs. 2 and 5c), as well as a lower percentage of CRAM (Fig. 2e and Supplementary Fig. 5e) and lower degradation index (Fig. 2f and Supplementary Fig. 5f) compared to shallower fluids with shorter DIC-based incubation times, further evidence for a distinct composition.

Global removal of marine DOC in cool crustal aquifers

High-temperature hydrothermal circulation through ridge axes accounts for the removal of $1.2 \pm 0.6 \times 10^9$ moles of refractory DOC per year[26], whereas warm (>20 °C) off-axis settings are thought to represent a much larger global DOC sink of $0.2–1.1 \times 10^{10}$ moles DOC per year[27]. These values, however, are less than 1% of the total observed DOC loss rate in the deep ocean[28]. Given that >90% of global hydrothermal fluid flux is probably hosted by older, cooler crust[29], low-temperature hydrothermal circulation, such as that studied here, has the potential to be a much larger net sink. The total flow rate of fluid through the volcanic crust below North Pond is not known, but thermal data and geometrical considerations provide general constraints. The seafloor heat flux through North Pond sediments is approximately 10–30% of lithospheric predictions[4,6]. Given the length scale of the flow from the outcrops to the crust under North Pond, the application of one-dimensional well-mixed aquifer calculations[30,31] suggests flow rates on the order of 10–100 m yr^{-1} (m^3 per year per m^2 of the cross-sectional crustal area (Supplementary Section 3)). For a simple flow-through crustal system under North Pond, this is equivalent to ~10^8 m^3 yr^{-1}. The global hydrothermal flux through cool crust is 4.8×10^{12} m^3 yr^{-1} (ref. [29]), equivalent to 10^4–10^5 North Pond systems. Based on the global hydrothermal fluid flux through cool crust, a DOC loss equivalent to that below North Pond yields a net removal of $0.8–1.2 \times 10^{11}$ mol DOC yr^{-1}, which is at least 5% of the total annual DOC loss within the ocean. The cool basalt-hosted subsurface, suitable for the establishment of substantial microbial populations, affords crustal microbes the opportunity to alter deep-ocean DOC over the entire residence time of the fluids. As fluids recovered from CORKs would have continued to circulate within the crustal flank of the Mid-Atlantic Ridge, the final inventory loss, and therefore the extrapolated global loss rate, could be even larger than we have calculated.

Our analyses underline the role that the subsurface microbial community plays in the degradation of aged organic matter, and support recent findings of a hidden reservoir of semilabile DOC within deep-ocean DOC[20]. They also illuminate the processes that occur in a fraction of crustal pore spaces that is normally unresolved in geophysical descriptions of hydrothermal fluid flow. They provide an opportunity to examine the molecular and isotopic characteristics of a remnant fraction of deep-ocean DOM that persists for an average of thousands of years in isolation from the open ocean. Environments such as the upper volcanic crust below North Pond play an important role in the global carbon cycle, and make a disproportionately large contribution towards maintaining the degraded molecular character and old radiocarbon age of deep-ocean DOC.

Methods

Methods, including statements of data availability and any associated accession codes and references, are available at https://doi.org/10.1038/s41561-018-0109-5.

References

1. Becker, K., Bartetzko, A. & Davis, E. E. Leg 174B Synopsis: Revisiting Hole 395A for logging and long-term monitoring of off-axis hydrothermal processes in young oceanic crust. In *Proc. IODP Sci. Results* (eds Becker, K. & Malone, M. J.) Vol. 174B (Integrated Ocean Drilling Progam Management International, 2001).
2. Villinger, H. in *Maria S. Merian Cruise Report MSM37* 1–42 (Senatskommission fur Ozeanographie, 2014).
3. Expedition 336 Scientists. Expedition 336 summary. In *Proc. IODP* (eds Edwards, K. J. et al.) Vol. 336, 101 (Integrated Ocean Drilling Progam Management International, 2012).
4. Schmidt-Schierhorn, F., Kaul, N., Stephan, S. & Villinger, H. Geophysical site survey results from North Pond (Mid-Atlantic Ridge). In *Proc. IODP* (eds Edwards, K. J. et al.) Vol. 336, 107 (Integrated Ocean Drilling Progam Management International, 2012).
5. Morin, R. H., Hess, A. E. & Becker, K. In situ measurements of fluid flow in DSDP Holes 395A and 534A: results from the DIANAUT Program. *Geophys. Res. Lett.* **19**, 509–512 (1992).
6. Langseth, M. G., Becker, K., Von Herzen, R. P. & Schultheiss, P. Heat and fluid flux through sediment on the western flank of the Mid-Atlantic Ridge: a hydrogeological study of North Pond. *Geophys. Res. Lett.* **19**, 517–520 (1992).
7. Meyer, J. L. et al. A distinct and active bacterial community in cold oxygenated fluids circulating beneath Mid-Atlantic seafloor. *Sci. Rep.* **6**, 22541 (2016).
8. Tully, B. J., Wheat, C. G., Glazer, B. T. & Huber, J. A. A dynamic microbial community with high functional redundancy inhabits the cold, oxic subseafloor aquifer. *ISME J.* **12**, 1–16 (2018).
9. Orcutt, B. N. et al. Oxygen consumption rates in subseafloor basaltic crust derived from a reaction transport model. *Nat. Commun.* **4**, 2539 (2013).
10. Fisher, A. T. in *Hydrogeology of the Oceanic Lithosphere* (eds Davis, E. E. & Elderfield, H.) 339–377 (Cambridge Univ. Press, Cambridge, 2004).
11. Fisher, A. T. & Becker, K. Channelized fluid flow in oceanic crust reconciles heat-flow and permeability data. *Nature* **403**, 71–74 (2000).
12. Dittmar, T., Koch, B., Hertkorn, N. & Kattner, G. A simple and efficient method for the solid-phase extraction of dissolved organic matter (SPE-DOM) from seawater. *Limnol. Ocean. Methods* **6**, 230–235 (2008).
13. Koch, B. P. & Dittmar, T. From mass to structure: an aromaticity index for high-resolution mass data of natural organic matter. *Rapid Commun. Mass Spectrom.* **20**, 926–932 (2006).
14. Flerus, R. et al. A molecular perspective on the ageing of marine dissolved organic matter. *Biogeosciences* **9**, 1935–1955 (2012).
15. LaRowe, D. E. et al. Identification of organic compounds in ocean basement fluids. *Org. Geochem.* **113**, 124–127 (2017).
16. Anderson, L. A. & Sarmiento, J. L. Redfield ratios of remineralization determined by nutrient data analysis. *Glob. Biogeochem. Cycles* **8**, 65–80 (1994).
17. Arnarson, T. S. & Keil, R. G. Mechanisms of pore water organic matter adsorption to montmorillonite. *Mar. Chem.* **71**, 309–320 (2000).
18. Lalonde, K., Mucci, A., Ouellet, A. & Gelinas, Y. Preservation of organic matter in sediments promoted by iron. *Nature* **483198**, 198–200 (2012).
19. Koch, B. P. & Dittmar, T. Erratum: from mass to structure: an aromaticity index for high-resolution mass data of natural organic matter. *Rapid Commun. Mass Spectrom.* **30**, 250 (2016).

20. Follett, C. L., Repeta, D. J., Rothman, D. H., Xu, L. & Santinelli, C. Hidden cycle of dissolved organic carbon in the deep ocean. *Proc. Natl Acad. Sci. USA* **111**, 16706–16711 (2014).

21. Hayes, J. M. Fractionation of the isotopes of carbon and hydrogen in biosynthetic processes. *Rev. Mineral. Geochem.* **43**, 225–278 (2001).

22. Loh, A. N., Bauer, J. E. & Druffel, E. R. M. Variable ageing and storage of dissolved organic components in the open ocean. *Nature* **430**, 877–881 (2010).

23. Hertkorn, N. et al. Characterization of a major refractory component of marine dissolved organic matter. *Geochim. Cosmochim. Acta* **70**, 2990–3010 (2006).

24. Berggren, M. & del Giorgio, P. A. Distinct patterns of microbial metabolism associated to riverine dissolved organic carbon of different source and quality. *J. Geophys. Res. Biogeosci.* **120**, 989–999 (2015).

25. Guillemette, F., McCallister, S. L. & del Giorgio, P. A. Differentiating the degradation dynamics of algal and terrestrial carbon within complex natural dissolved organic carbon in temperate lakes. *J. Geophys. Res. Biogeosci.* **118**, 963–973 (2013).

26. Hawkes, J. A. et al. Efficient removal of recalcitrant deep-ocean dissolved organic matter during hydrothermal circulation. *Nat. Geosci.* **8**, 856–860 (2015).

27. Lang, S. Q., Butterfield, D. A., Lilley, M. D., Johnson, H. P. & Hedges, J. I. Dissolved organic carbon in ridge-axis and ridge-flank hydrothermal systems. *Geochim. Cosmochim. Acta* **70**, 3830–3842 (2006).

28. Hansell, D. A., Carlson, C. A., Repeta, D. J. & Schlitzer, R. Dissolved organic matter in the ocean: a controversy stimulates new insights. *Oceanography* **22**, 202–211 (2009).

29. Johnson, H. P. & Pruis, M. J. Fluxes of fluid and heat from the oceanic crustal reservoir. *Earth Planet. Sci. Lett.* **216**, 565–574 (2003).

30. Langseth, M. G. & Herman, B. M. Heat transfer in the oceanic crust of the Brazil Basin. *J. Geophys. Res.* **86**, 10805–10819 (1981).

31. Rosenberg, N. D., Fisher, A. T. & Stein, J. S. Large-scale lateral heat and fluid transport in the seafloor: revisiting the well-mixed aquifer model. *Earth Planet. Sci. Lett.* **182**, 93–101 (2000).

32. Stuiver, M. & Polach, H. A. Reporting of ^{14}C data. *Radiocarbon* **19**, 355–363 (1977).

33. Pohlman, J. W., Bauer, J. E., Waite, W. F., Osburn, C. L. & Chapman, N. R. Methane hydrate-bearing seeps as a source of aged dissolved organic carbon to the oceans. *Nat. Geosci.* **4**, 37–41 (2011).

34. McCarthy, M. D. et al. Chemosynthetic origin of ^{14}C-depleted dissolved organic matter in a ridge-flank hydrothermal system. *Nat. Geosci.* **4**, 32–36 (2011).

Author contributions

S.R.S.W., U.J., P.R.G. and J.A.H. formulated the original hypotheses and designed the project, S.R.S.W., U.J., H.O., T.D. and P.R.G. collected samples, performed research and participated in the data analysis and data interpretation. A.T.F. provided fluid-flow calculations and constraints. All the authors discussed the data presented in this manuscript and participated in its writing.

Competing interests

The authors declare no competing interests.

Additional information

Supplementary information is available for this paper at https://doi.org/10.1038/s41561-018-0109-5.

Reprints and permissions information is available at www.nature.com/reprints.

Correspondence and requests for materials should be addressed to S.R.S. or T.D. or P.R.G.

Publisher's note: Springer Nature remains neutral with regard to jurisdictional claims in published maps and institutional affiliations.

Methods

Sample locations and description. Fluids were recovered from 90–120 m below the sea floor (mbsf) at IODP Hole U1382A (46° 04.8911′ W, 22° 45.3531′ N), where 90 m of sediment have accumulated over the basalt crust (Fig. 1b,c)[35], and three depths (70–146 mbsf, 146–200 mbsf and 200–332 mbsf) from IODP Hole U1383C (46° 03.1662′ W, 22° 48.1241′ N) under 38 m of sediment (Fig. 1b,c)[36]. Deep-Atlantic bottom water was collected from a conductivity–temperature–depth (CTD) cast (46° 03.1700′ W, 22° 48.1200′ N) at 4,400 m water depth in 2012 and a CTD cast (46° 03.6700′ W, 22° 47.3200′ N) at 4,465 m water depth in 2014. Sediment samples for a comparative analysis of pore-water SPE-DOM by FT-ICR-MS were collected from IODP Holes U1382B (46° 04.8748′ W, 22° 45.3528′ N (approximately 30 m from U1382A)), U1383D (46° 03.1628′ W, 22° 48.1316′ N (approximately 15 m from U1383C)) and U1384A (46° 05.3464′ W, 22° 48.7086′ N) during IODP Expedition 336 in October 2011 (Fig. 1b)[37].

Sample collection. Crustal fluids and deep-Atlantic bottom water were collected during postdrilling cruises in April 2012 and March–April 2014 on the research vessel (RV) *Maria S. Merian* using the remotely operated underwater vehicle (ROV) *Jason II*. Detailed descriptions of sample retrieval are published[7]. Briefly, fluids were pumped directly into 15 l gas-tight, foil-lined Tedlar sample bags (Jensen Inert Products), which were precleaned with 10% HCl and sterilized by gamma irradiation prior to deployment. Once aboard, the crustal aquifer fluid samples were transferred immediately into precombusted 120 ml serum vials (2012), precombusted 2 l Schott bottles (2012) or precombusted 1 l Schott bottles (2014) flushed sequentially with a 10% HCl solution, distilled water and 70% ethanol, followed by a rinse with distilled water for three minutes each by a peristaltic pump. Serum bottles (120 ml) were sealed with 10% HCl-rinsed silicone stoppers and frozen at −80 °C until further processing for FT-ICR-MS analysis. Schott bottles were filled to overflowing, sealed such that no headspace remained with 10% HCl-rinsed polytetrafluoroethylene (PTFE)-lined screw caps and stored at 5 °C for isotope analysis of the DIC and DOC until subsampled on shore. Deep-Atlantic bottom water collected in 2012 for FT-ICR-MS analysis was stored at −80 °C in 10% HCl-rinsed 60 ml high-density polyethylene bottles. Deep-Atlantic bottom water was collected for isotopic analysis in 2014 and stored at 5 °C in precombusted glass Schott bottles until subsampled.

Sediment samples for pore water analysis were collected from IODP Holes U1382B, U1383D and U1384A during Expedition 336 on the *JOIDES Resolution* in October 2011. Locations and site descriptions are provided in Fig. 1b,c and a previous publication[37]. Fluorescent microspheres were used to control for contamination during drilling. Retrieved sediment cores were handled using sterile and clean-room techniques to avoid contamination during the sample processing. Whole round sediment cores were frozen at −80 °C and shipped in refrigerated containers to the IODP archives in Bremen and Texas. Detailed descriptions of the sediment sampling procedures are reported in the IODP Expedition 336 Methods[38]. Sediment samples for this study were requested from the IODP archives and shipped on dry ice. Samples were thawed on precombusted aluminium foil at 4 °C for 15 h, and then transferred into plastic centrifugation containers that were prerinsed with 10% HCl and distilled water. Samples were centrifuged for 30 min at a low speed. The supernatant was transferred into precombusted glass bottles and sealed with 10% HCl-rinsed, PTFE-lined caps. The supernatant was stored at −20 °C until further processing for FT-ICR-MS analysis.

DOC concentration, Δ^{14}C and δ^{13}C analyses of DIC and DOC. Fluids in glass Schott bottles were subsampled for radiocarbon analysis at the National Ocean Sciences Accelerator Mass Spectrometry (NOSAMS) Facility in an N_2-filled glove bag using sterile techniques. For DIC analysis, 200 ml of fluid was subsampled into precombusted glass bottles with precombusted glass stoppers and ground-glass joints, poisoned with mercuric chloride and preserved as per standard NOSAMS protocol (http://www.whoi.edu/fileserver.do?id=75006&pt=2&p=75096, accessed in 2013). For DOC analysis, fluids (90 ml) were subsampled into precombusted amber glass bottles, sealed with PTFE-lined caps and frozen at −40 °C until the analysis.

DOC concentrations were determined by manometric quantification of CO_2 evolved during ultraviolet photo-oxidation[39]. Our DOC concentrations are similar to although systematically lower than those reported by Meyer et al.[7] from high-temperature combustion catalytic oxidation on the same fluids. We note that, although lower than the value (50 ± 1 μM) reported by Meyer et al.[7], our value for bottom water (41 ± 2 μM) is similar to regional estimates of the DOC concentration in the deep North Atlantic (40–42 μM (refs [28,40]).

Radiocarbon and stable carbon isotopic analysis was performed at NOSAMS. ΣCO_2 was extracted from DIC samples after acidification[41] and the total organic carbon from DOC samples by ultraviolet oxidation[39]. δ^{13}C values were determined on a split of sample CO_2 by dual-inlet isotope ratio mass spectrometry, and the remainder of the CO_2 was converted into graphite for radiocarbon analysis by accelerator mass spectrometry. Ongoing analysis of the reproducibility across all sample types at NOSAMS indicates a measurement uncertainty for $\delta^{13}C_{DIC}$ of ± 0.05‰ (refs [42,43]). Uncertainty is reported individually for Δ^{14}C values. DOC sample results are all corrected for process blanks using published methods[44,45]. The measurements of modern and dead standards indicate that processing introduces the equivalent of 0.21 ± 0.2 μmol modern carbon and 0.33 ± 0.3 μmol dead carbon. We observe an overall reproducibility of ± 0.3‰ for $\delta^{13}C_{DOC}$ and ± 7–10‰ for relatively modern $\Delta^{14}C_{DOC}$ of the range measured in this study.

FT-ICR-MS analysis of SPE-DOM. The molecular composition of the DOM in bottom seawater, crustal aquifer fluids and sediment pore waters was analysed using ultrahigh-resolution FT-ICR-MS. Samples were thawed at 4 °C, then acidified to pH 2 before the DOM was extracted by solid-phase extraction on styrene-divinylbenzene polymer columns (Agilent PPL), as described elsewhere[12,46]. Due to the exceptionally small sample sizes and low DOC concentrations, extraction efficiencies on a carbon basis were not determined using standard methods. Approximate extraction efficiencies were 30–50% for aquifer fluids. The extracted SPE-DOM was analysed using a soft electrospray ionization technique in the negative mode on a Bruker Daltonics 15 Tesla Solarix FT-ICR mass spectrometer in a dilution of 1:1 (v/v) with ultrapure water. Every sample was measured five times (except CTD bottom-water samples, $n = 4$) and for each measurement 600 broadband scans were accumulated. All the detected compounds had a molecular mass between 154 and 973 Da. The obtained mass spectra were internally calibrated and molecular formulae were assigned to peaks with a minimum signal-to-noise ratio of five and for a maximum elemental combination of $C_{40}H_{80}O_{40}N_4P_1S_2$, which allows a mass tolerance of 0.5 ppm. Thereafter, molecular formulae detected in the process blanks with a minimum signal-to-noise ratio of ten were considered contaminations and excluded from further analyses. Also excluded were those masses that occurred in fewer than five analyses between all samples ($n = 89$). Within our 89 SPE-DOM samples (including replicate analyses), we identified 9,207 unique molecular formulae in total; 880–5,731 molecular formulae were detected per sample, but most of the variability in numbers of formulae was observed in sediment (880–3,874 formulae) rather than bottom water and aquifer fluids (4,115–5,731 formulae).

SPE-DOM molecular indices were calculated using normalized FT-ICR-MS signal intensities. AI_{mod} was calculated using a published method[13,19]:

$$AI_{mod} = \frac{DBE_{AI}}{C_{AI}} = \frac{1 + C - \frac{1}{2}O - S - \frac{1}{2}(N + P + H)}{C - \frac{1}{2}O - N - S - P} \tag{1}$$

where DBE is the double-bond equivalent and C, O, H, S, N and P are the numbers of the respective elements. The degradation index, I_{DEG}, described elsewhere[14], was calculated as:

$$I_{DEG} = \frac{\sum (\text{magnitudes NEG}_{I_{DEG}})}{\sum (\text{magnitudes NEG}_{I_{DEG}} + POS_{I_{DEG}})} \tag{2}$$

where compounds that correlate negatively with ageing ($NEG_{I_{DEG}}$) have molecular formulae $C_{21}H_{26}O_{11}$, $C_{17}H_{20}O_9$, $C_{19}H_{22}O_{10}$, $C_{20}H_{22}O_{10}$ and $C_{20}H_{24}O_{11}$, and positively correlating compounds ($POSI_{DEG}$) have molecular formulae $C_{13}H_{18}O_7$, $C_{14}H_{20}O_7$, $C_{15}H_{22}O_7$, $C_{15}H_{22}O_8$ and $C_{16}H_{24}O_8$.

The proportion of CRAM molecules was calculated as occupying the ranges of DBE/C = 0.30–0.68, DBE/H = 0.20–0.95 and DBE/O = 0.77–1.75 (ref. [23]).

A Bray–Curtis[47] dissimilarity matrix was calculated based on all replicate analyses and the respective detected relative FT-ICR-MS signal intensities to identify patterns of change in the molecular SPE-DOM composition. A complete linkage was used to cluster Bray–Curtis dissimilarities. All the analyses were performed using R (version 3.3.1) and the vegan software package[48].

Data availability. The authors declare that all data supporting the findings of this study are available within the article and its Supplementary Information tables. We additionally use dissolved oxygen, DOC concentrations and DIC Δ^{14}C data from the CLIVAR and Carbon Hydrographic Data Office, Hydrographic Cruise 318M200406 along Line A20 in 2012 (https://cchdo.ucsd.edu/cruise/318M200406) and Hydrographic Cruise 316N20111106 along Line GT11 in 2012 (https://cchdo.ucsd.edu/cruise/316N20111106).

References

35. Expedition 336 Scientists. Site U1382. In *Proc. IODP* (eds Edwards, K. J. et al.) Vol. 336, 104 (Integrated Ocean Drilling Progam Management International, 2012).
36. Expedition 336 Scientists. Site U1383. In *Proc. IODP* (eds Edwards, K. J. et al.) Vol. 336, 105 (Integrated Ocean Drilling Progam Management International, 2012).
37. Expedition 336 Scientists. Sediment and basement contact coring. In *Proc. IODP* (eds Edwards, K. J. et al.) Vol. 336, 106 (Integrated Ocean Drilling Progam Management International, 2012).
38. Expedition 336 Scientists. Methods. In *Proc. IODP* (eds Edwards, K. J. et al.) Vol. 336, 102 (Integrated Ocean Drilling Progam Management International, 2012).

39. Beaupré, S. R., Druffel, E. R. M. & Griffin, S. A low-blank photochemical extraction system for concentration and isotopic analyses of marine dissolved organic carbon. *Limnol. Oceanogr. Methods* **5**, 174–184 (2007).

40. McCartney, M. & Gong, D. *WOCE A20 Hydrographic Cruise: 33AT20120419 Bottle Data* (CCHDO, 2012); https://cchdo.ucsd.edu/cruise/33AT20120419

41. McNichol, A. P., Jones, G. A., Hutton, D. L. & Gagnon, A. R. The rapid preparation of seawater ΣCO₂ for radiocarbon analysis at the National Ocean Sciences AMS facility. *Radiocarbon* **36**, 237–246 (1994).

42. Elder, K. L., McNichol, A. P. & Gagnon, A. R. Reproducibility of seawater, inorganic and organic carbon ^{14}C results at NOSAMS. *Radiocarbon* **40**, 223–230 (1998).

43. Jenkins, W. J., Elder, K. L., McNichol, A. P. & von Reden, K. F. The passage of the bomb radiocarbon pulse into the Pacific Ocean. *Radiocarbon* **52**, 1182–1190 (2010).

44. Currie, L. A. et al. Low-level (submicromole) environmental ^{14}C metrology. *Nucl. Instrum. Methods Phys. Res. Sect. B* **172**, 440–448 (2000).

45. Santos, G. M. et al. Blank assessment for ultra-small radiocarbon samples: chemical extraction and separation versus AMS. *Radiocarbon* **52**, 1322–1335 (2010).

46. Rossel, P. E., Vähätalo, A. V., Witt, M. & Dittmar, T. Molecular composition of dissolved organic matter from a wetland plant (*Juncus effusus*) after photochemical and microbial decomposition (1.25 yr): common features with deep sea dissolved organic matter. *Org. Geochem.* **60**, 62–71 (2013).

47. Bray, J. R. & Curtis, J. T. An ordination of the upland forest community of southern Wisconsin. *Ecol. Monogr.* **27**, 325–349 (1957).

48. Oksanen, J. et al. vegan: Community Ecology Package. R package version 2.3-1 (2015); http://cran.r-project.org/package=vegan